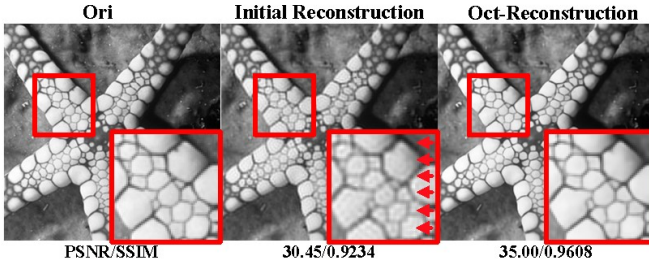


Supplementary Material for “AutoBCS: Block-based Image Compressive Sensing with Data-driven Acquisition and Non-iterative Reconstruction”

I. EXTENDED ABLATION STUDY

The influences of the octave reconstruction subnetwork and generated LSM on the performance of the proposed AutoBCS framework are investigated; and AutoBCS for color images is also studied in this extended Section.

As depicted in the paper, the initial reconstruction subnetwork is essential and indispensable in the proposed AutoBCS framework; however, the effectiveness of the octave reconstruction subnetwork has not yet been verified. Supplementary Fig. 1 illustrates the output images from each sub-network, showing that the octave reconstruction subnetwork can significantly alleviate artifacts and improve image quality. Overall, both reconstruction subnetworks are essential in the proposed AutoBCS framework. Without the initial reconstruction subnetwork, \mathbf{x}_i cannot be directly reconstructed by the octave reconstruction subnetwork from the measurement vector \mathbf{y}_i , while there would be heavy artifacts in the reconstruction results if there were no octave reconstruction subnetwork.



Supplementary Fig. 1. Comparison of the results restored from the initial and octave reconstruction sub-networks of AutoBCS at $\tau = 0.25$. Red arrows point to the blocking artifacts in the initial reconstruction output.

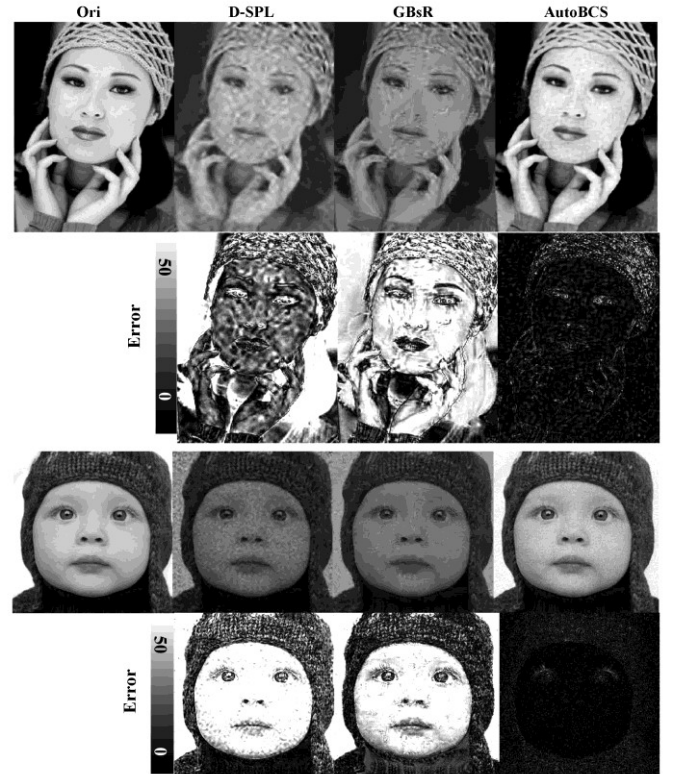
A comparative experiment is designed to elucidate the importance of the generated LSM for the proposed AutoBCS scheme. A variant of AutoBCS, called AutoBCS(GSM), is obtained by using a fixed GSM instead of using the LSM, and it is trained with the same training datasets as before with the same training parameters. A comparison between the variant version and the original AutoBCS on an image at $\tau = 0.1$ is shown in Supplementary Fig. 2. Moreover, we have compared the proposed AutoBCS and the traditional BCS reconstruction algorithms (including IRLS, D-SPL, MH-SPL, WaPT, and GBsR) with our generated LSM on three typical benchmark databases, i.e., Set5, Set14, and BSD100, as shown in SUPPLEMENTAL TABLE I. According to these results, the generated LSM can not only significantly enhance the quality

of reconstructed images from both the initial and octave reconstruction subnetworks, but also improve the recovery performance of traditional BCS reconstruction methods.

Moreover, our proposed AutoBCS can be directly applied to color images. For example, we can use our trained AutoBCS models on the RGB color space for the color images ‘Peppers’, ‘Tiger’, ‘Dock’, and ‘Desert’ at different sampling rates, as shown in Supplementary Fig. 3. For color image ‘Peppers’, the PSNR/SSIM values are 34.41/0.8726, 33.85/0.8641, 31.49/0.8155, 28.92/0.7625, 24.41/0.6452 at the sampling rate of 0.3, 0.25, 0.1, 0.04, 0.01, respectively. Supplementary Fig. 3 verifies that the proposed AutoBCS contains rich semantic content even at a particularly low sampling rate. Overall, it shows that AutoBCS achieves comparable results on color images as it does on gray images.

II. EXTENDED FIGURE

A. Extended Figure 1

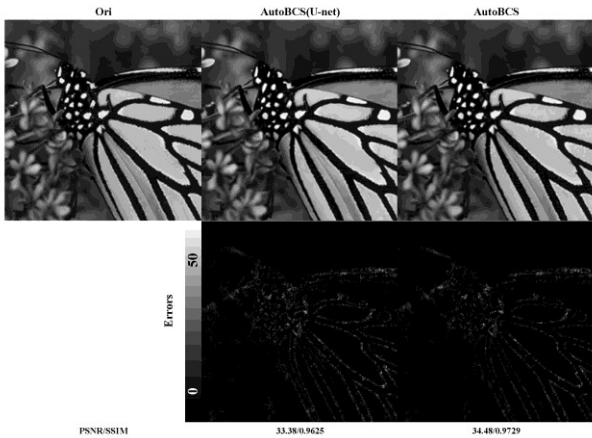


Extended Fig. 1. Comparison of noisy image reconstruction for traditional BCS approaches (D-SPL and GBsR) and AutoBCS on Set5 in case of $\tau = 0.1$ with Gaussian noise of $\sigma_n = 0.1$, where the second and the fourth rows are corresponding image errors. Please zoom in for better comparison.



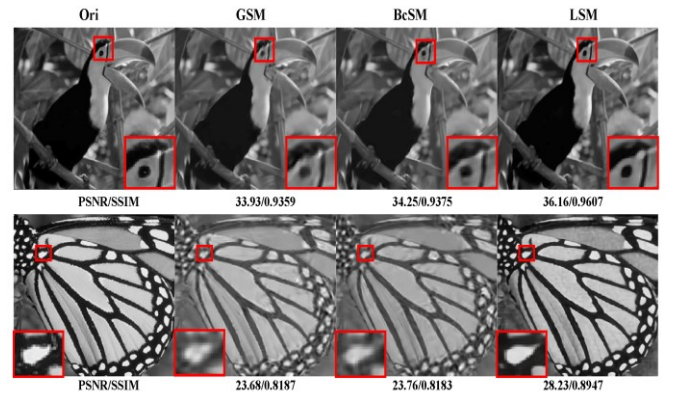
Supplementary Fig. 2. Comparison of the reconstruction images from both the initial and octave reconstruction sub-networks for AutoBCS(GSM) and AutoBCS at $\tau = 0.1$. Please zoom in for better comparison.

B. Extended Figure 2

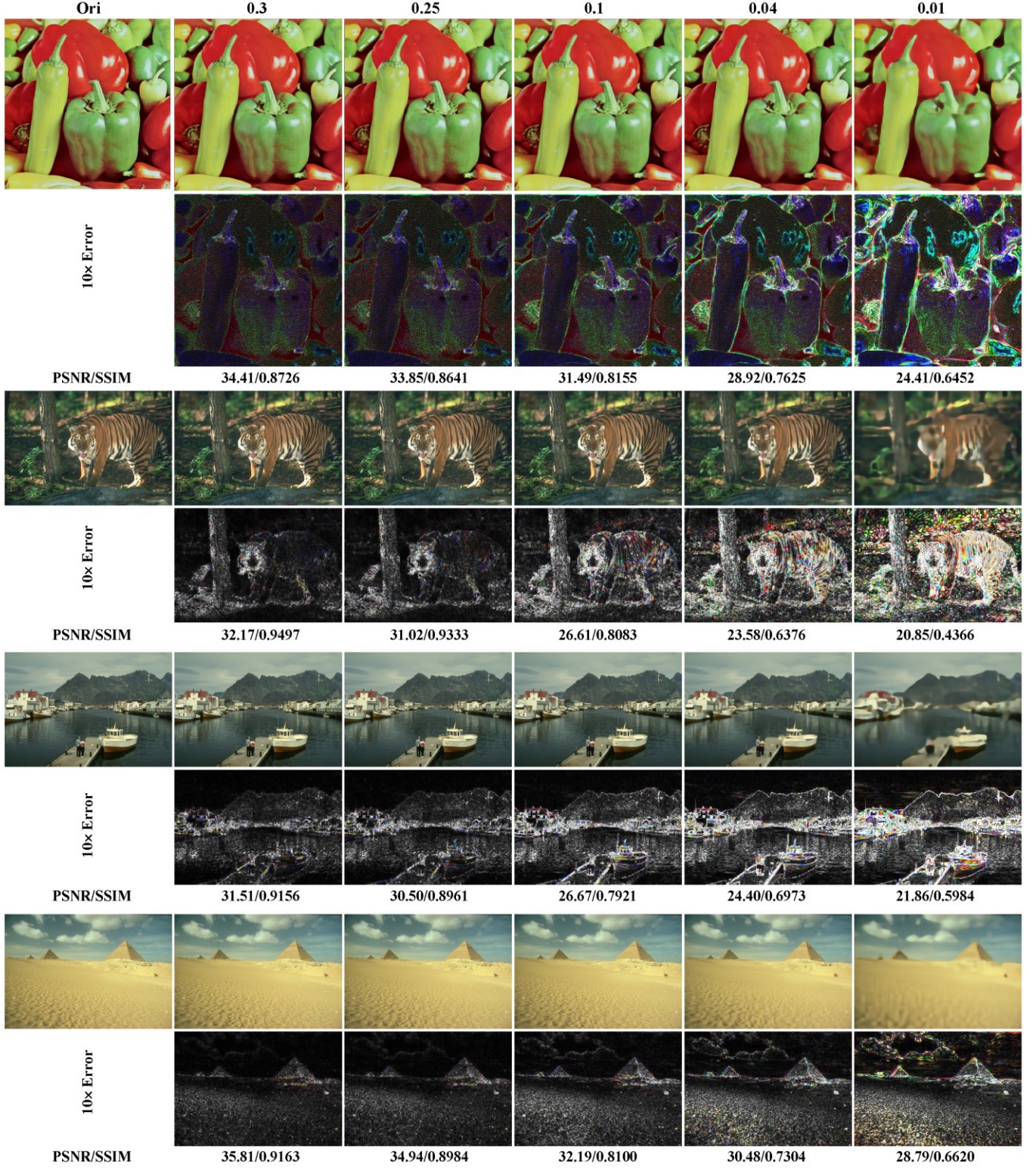


Extended Fig. 2. Comparison of the reconstruction images for Auto-BCS(U-net) and the original AutoBCS at $\tau = 0.25$.

C. Extended Figure 3



Extended Fig. 3. Comparison of image reconstruction using three sensing matrices combined with traditional GBR algorithm. First column: the original image; the reconstruction columns are based on GSM, BcSM and our trained LSM, respectively. Please zoom in for better comparison.



Supplementary Fig. 3. Illustration of reconstructed color images by using AutoBCS at different sampling rates. The first column: original image; the reconstruction columns for left to right correspond to $\tau = 0.3$, $\tau = 0.25$, $\tau = 0.1$, $\tau = 0.04$, and $\tau = 0.01$, respectively. Please zoom in for better comparison.

SUPPLEMENTAL TABLE I: AutoBCS vs. different conventional BCS methods with our generated LSM on three typical benchmark databases

Database	Sampling rate τ	IRLS		D-SPL		MH-SPL		WaPT		GBsR		AutoBCS	
		SSIM	PSNR	SSIM	PSNR	SSIM	PSNR	SSIM	PSNR	SSIM	PSNR	SSIM	PSNR
Set5	0.01	0.5124	20.21	0.3552	18.30	0.5947	22.62	0.6152	23.10	0.6278	23.79	0.6696	24.25
	0.04	0.7320	26.45	0.6514	24.90	0.7792	27.48	0.7921	27.95	0.8045	28.29	0.8446	29.18
	0.1	0.8463	29.87	0.8375	29.86	0.8499	30.89	0.8892	31.58	0.9002	32.51	0.9190	33.28
	0.25	0.9401	34.56	0.9355	33.58	0.9455	35.74	0.9518	36.11	0.9544	36.62	0.9607	37.65
	0.3	0.9530	36.01	0.9515	35.34	0.9549	36.72	0.9610	37.08	0.9627	37.74	0.9675	38.75
	Avg.	0.7968	29.42	0.7462	28.40	0.8248	30.69	0.8419	31.16	0.8499	31.79	0.8723	32.62
Set14	0.01	0.5014	20.86	0.4553	18.63	0.5366	21.83	0.5512	22.07	0.5626	22.66	0.5968	23.12
	0.04	0.6651	25.10	0.5725	22.41	0.6840	25.53	0.6954	25.78	0.7063	26.05	0.7348	28.67
	0.1	0.8107	28.04	0.7320	25.17	0.8011	28.33	0.8108	28.64	0.8180	28.80	0.8343	29.56
	0.25	0.8958	31.12	0.9029	31.53	0.9055	32.29	0.9114	32.76	0.9162	32.93	0.9205	33.67
	0.3	0.9149	32.85	0.9185	32.56	0.9220	33.32	0.9287	33.89	0.9322	34.07	0.9347	34.81
	Avg.	0.7576	27.59	0.7162	26.06	0.7698	28.26	0.7795	28.63	0.7871	28.90	0.8042	29.97
BSD100	0.01	0.4987	21.42	0.4163	19.22	0.5159	22.73	0.5279	23.07	0.5385	23.48	0.5578	23.79
	0.04	0.6215	24.65	0.5271	22.87	0.6419	25.54	0.6578	25.69	0.6631	25.98	0.6833	26.40
	0.1	0.7602	27.70	0.6647	25.66	0.7607	27.77	0.7724	27.95	0.7784	28.15	0.7937	28.74
	0.25	0.8814	30.98	0.8750	30.29	0.8809	31.13	0.8957	31.41	0.8942	31.65	0.9019	32.33
	0.3	0.8998	32.05	0.8966	31.41	0.9028	32.12	0.9089	32.38	0.9148	32.69	0.9215	33.39
	Avg.	0.7323	27.36	0.6759	25.89	0.7404	27.86	0.7525	28.10	0.7578	28.39	0.7716	28.93

D. Extended Figure 4

Extended Fig. 4. Illustration of reconstructed images by using AutoBCS at different sampling rates. The first column: original image; the reconstruction columns for left to right correspond to $\tau = 0.3$, $\tau = 0.25$, $\tau = 0.1$, $\tau = 0.04$, and $\tau = 0.01$, respectively. Please zoom in for better comparison.